

Using Clustering and APS Method Performance Improvement of Cell Free Massive MIMO System

<https://doi.org/10.59879/maTjD>

Panpan Yin¹, Tasher Ali Sheikh²

School of Engineering, Guangzhou College of Technology and Business, Foshan City, Guangdong Province, China¹

Department of Electronics and Telecommunication Engineering, Residential Girls' Polytechnic, Golaghat, Assam, India-785702²
tasher.ece@gmail.com

Abstract: Recently Cell Free massive multiple input multiple output (M-MIMO), comprising of large number of distributed access points (APs) is a promising technology in order to provide high data rate, spectral efficiency (SE), and energy efficiency (EE). In order to achieve optimality in the performance of the cell free M-MIMO, a suitable selection technique of AP is performed among large number of AP. In this work, zero-forcing (ZF) and minimum means square error (MMSE) linear precoding are used since it is free from self-interference hence, improving the system sum-rate. The present work proposes a maximum channel gain-based Access Point Selection (APS) algorithm for access point (AP) selection in the Cell free M-MIMO network in order to enhance the system data-rate. Using APS algorithm, it is proposed to select those APs whose channel gain is highest therefore it automatically improves the rate of the system. The same number of users is scheduled using a simple semi-orthogonal user scheduling (SUS) algorithm. We also used a user clustering algorithm for grouping the users around the AP to schedule the best users. It is observed from the results that the APS and SUS algorithm jointly improve the system rate significantly in cell free massive MIMO systems.

Keywords— Cell Free Massive MIMO; User Clustering; User Scheduling; Access Point Selection.

I. Introduction

In upcoming days future wireless networks have to manage at a time billions of devices where each of the users' needs a high throughput in order to support many applications such as voice, real-time video, high quality movies, etc. Cellular networks could not handle such huge connections since user terminals at the cell boundary suffer from very high interference, and hence, perform badly. Furthermore, conventional cellular systems are designed mainly for human users. In future wireless networks, machine-type

communications such as the Internet of Things, Internet of Everything, Smart X, massive device-to-device (D2D) and machine-to-machine (M2M) communications, etc. are expected to play an important role. The main challenges of machine-type communications are scalability and efficient connectivity for billions of devices. Centralized technology with cellular topologies does not seem to be working for such scenarios since each cell can cover a limited number of user terminals. So why not cell free (CF) structures with decentralized technology? Therefore, to serve many user terminals and to simplify the signal processing in a distributed manner, M-MIMO technology is added now a days. The combination between CF structure and M-MIMO technology yields a new concept which is called CF M-MIMO. Recently, CF M-MIMO has been introduced as a practical and useful embodiment of the network MIMO concept [1]. In CF M-MIMO, a large number of APs equipped with single or multiple antennas, and distributed over a large area, coherently serving a large number of users in the same time-frequency resource.

In CF M-MIMO networks all APs cooperate via a backhaul network exchanging information with a central processing unit (CPU). As the traditional M-MIMO [2], CF M-MIMO exploits the favourable propagation and channel hardening properties when the number of APs is large to multiplex many users in the same time-frequency resource with small inter-user interference (IUI). Thus, it can offer a huge SE with simple signal processing. More importantly, in a CF M-MIMO configuration, the service antennas are brought close to the users, which yields a high degree of macro-diversity and low path losses [1]; hence, many users can be served simultaneously with uniformly good quality of service (QoS). Furthermore, it was shown in [1] that CF M-MIMO performed simultaneously well than the conventional small-cell systems, where each user is served by a single AP. For these reasons, CF M-MIMO is considered EE promising technology for next generation wireless systems. Despite its potential, however, besides [1] there is fairly little

work on CF M-MIMO available in the literature. In [3], the performance of CF M-MIMO with zero forcing (ZF) processing was analysed, under the assumption that all pilot sequences assigned to the users were mutually orthogonal. CF M-MIMO with beamformed downlink training was investigated in [4]. The conclusion was that by beamforming the pilots, the performance of the CF M-MIMO downlink can be substantially improved.

A compute-and-forward approach for CF M-MIMO to reduce the backhaul load was proposed and analysed in [5]. All the above-cited works assumed that the APs have only a single antenna. However, the APs can be equipped with multiple antennas to increase the diversity and array gains, as well as, reduce the backhaul requirements. In addition, while it is well-known that traditional M-MIMO is EE [6], it is not yet clear how good the EE of CF M-MIMO is. The argument is that in CF M-MIMO, more backhaul links are required which potentially increase the total power consumption to such a level that can overwhelm the SE gains.

In this paper, we used ZF and MMSE linear precoding schemes for signal processing. In these two precoding schemes, the weighted vectors are chosen to avoid interferences among the users and usually, these are power inefficient as the weight vectors are not matched to user channels. But, when the number of users N is significantly large, it provides a huge system sum-rate. This happens because of multiuser diversity [12]. The systematic block diagram of our proposed cell free massive MIMO system is shown in figure-3. The major contributions of this paper summarized as follows:

- i. Using simple K -means clustering, a large number of users are separated into equal number of AP in the considered area.
- ii. Semi-orthogonality User Selection (SUS) algorithm is used to schedule the best users from each cluster.
- iii. Access Points are selected based on maximum channel gain.
- iv. ZF and MMSE linear precoding schemes are used to reduce interference and enhanced the system rate.

The rest of this paper is ordered as follows. Section-II, present the system model. We report the linear precoding in section-III. User grouping is described in section-IV; User scheduling algorithm are explained in detail in section-V and Access Point Selection (APS) algorithm is described in section VI. Calculation of computational complexity of SUS algorithm are explained in detail in section-VII. The simulation results and discussion are explained in section-VIII and section-IX concluded this paper.

Notations: In the paper, unless otherwise specified, bold lower case, bold upper case, and upper case are used to represent vectors, matrices, and sets, respectively. Correspondingly $\mathcal{CN}(0, \sigma^2)$ represents the complex Gaussian distribution with zero mean and unit variance. $(\cdot)^H$ is the Hermitian of the matrix, $(\cdot)^T$

is transposed, $(\cdot)^\dagger$ is the Moore Penrose Pseudo-inverse and $\text{tr}(\cdot)$ is the trace of the matrix.

II. System Model

We assume a CF M-MIMO system which comprises of M APs that serve simultaneously in a fully-cooperative fashion N users, equipped each with a single omni-directional antenna in TDD mode which means that the uplink and downlink channels are reciprocal of each other as depicted in Figure 1. Additionally, we considered that the number of APs is much larger than the number of users i.e., $M \gg N$. All users are arbitrarily distributed over a relatively large geographical area. Initially, all users and APs are allocated a single antenna randomly in the vast area along with the assumption that all APs are randomly located throughout the area and are assumed to have imperfect CSI. The APs and the users are also considered to be perfectly synchronized in both time and frequency. Moreover, we suppose that the APs are managed by a central processing unit (CPU) to which they are linked through a back-haul link. The CPU can handle part of the physical layer information process such as data coding and decoding.

The channel of a user is assumed to be frequency-flat slow fading on each orthogonal frequency division multiplexing (OFDM) subcarrier. In the sequel, the subcarrier index will be omitted for the sake of simplicity. Let $\mathbf{g}_{mn} \in \mathbb{C}^{N \times 1}$, denote the complex channel vector between the n^{th} user and the m^{th} AP. It can be modeled as follows-

$$\mathbf{g}_{mn} = \sqrt{\beta_{mn}} \mathbf{h}_{mn} \quad (1)$$

where $\mathbf{h}_{mn} \approx \mathcal{CN}(0, \mathbf{I}_N)$ with \mathbf{I}_N being the $N \times N$ identity matrix, $m = 1, \dots, M$, $n = 1, \dots, K$, denote the small scale fading coefficients which are independent and identically distributed (i.i.d) while β_{mn} , $m = 1, \dots, M$, $n = 1, \dots, K$, the large-scale fading coefficients that include path-loss exponent and shadow fading variance.

a. Uplink pilot-based channel estimation

The system is working according to a TDD protocol. Each coherence interval T_c is divided between uplink training and downlink data transmission. By exploiting uplink/downlink channel reciprocity [7], the downlink CSI can be estimated through uplink training. During the uplink training phase, each user is assigned a training sequence that spans $\tau < T_c$ channel uses. The pilot sequences used in the channel estimation phase can be represented by a matrix $\Phi \in \mathbb{C}^{\tau \times N}$. The k^{th} column of the matrix denoted by $\Phi_k \in \mathbb{C}^{\tau \times 1}$ account for the pilot sequence used by the k^{th} user. Each element of Φ_k is of unit magnitude so that it has a constant power level $\|\Phi_k\|^2 = \tau$. The channel estimate can be obtained in a decentralized fashion at each AP m . Define $\mathbf{g}_{mn} \triangleq [\mathbf{g}_{m1}, \dots, \mathbf{g}_{mn,k}]$, the $N \times K$ received pilot matrix signal at the m^{th} AP is expressed as

$$\mathbf{Y}_{m,p} = \sqrt{\tau \rho_p} \mathbf{G}_m \Phi^\dagger + \omega_{m,p} \quad (2)$$

where ρ_p is the transmit power during the training phase, and $\omega_{m,p} \in \mathbb{C}^{N \times K}$ is the complex additive white Gaussian noise (AWGN) matrix at the m^{th} AP. The elements of $\omega_{m,p}$ are i.i.d. random variables that follow a standard normal distribution.

The m^{th} AP can perform MMSE [8] estimation of $\mathbf{g}_{m,n}$ to obtain the corresponding channel estimate, $\hat{\mathbf{g}}_{m,n}$ which is given by [9]

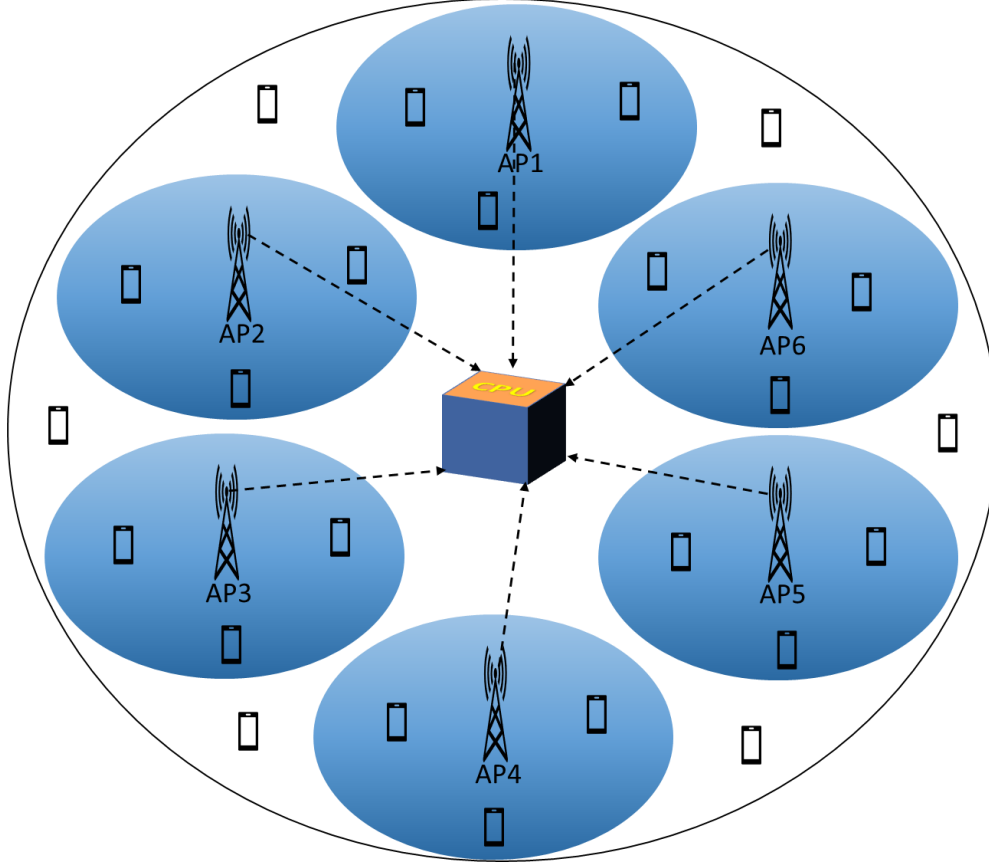


Figure-1: Cell-Free Massive MIMO system

$$\hat{\mathbf{g}}_{m,k} = \frac{\sqrt{\tau\rho_p}\beta_{mn}}{\tau\rho_p \sum_{j=1}^N \beta_{mj} |\Phi_k^H \Phi_j|^2 + 1} \times \left(\sqrt{\tau\rho_p} \mathbf{g}_{mk} + \sqrt{\tau\rho_p} \sum_{j=1, j \neq k}^K \mathbf{g}_{mj} \Phi_k^H \Phi_j + \omega_{m,k} \right) \quad (3)$$

where $\omega_{m,k} \approx \mathcal{CN}(0,1)$ is the k^{th} column of the matrix $\omega_{m,p} \Phi$. The quality of the channel estimation is captured through the minimum mean-squared error (MMSE) $\mathbb{E} \{ \|\mathbf{g}_{mk} - \hat{\mathbf{g}}_{m,k}\|^2 \}$. A good estimation quality is usually represented by a small MMSE. Also, the channel estimate in (3) is corrupted by pilot signals sent by other users, in case $K > \tau$, leading to pilot contamination which degrades user's achievable rate [10]. It is worth mentioning that, we only assume a given transmit power ρ_p during each training phase as this paper does not focus on the impact of adjusting ρ_p on the quality of channel estimates. Similar to [11], this paper assumes imperfect channel reciprocity. Denote $\tilde{\mathbf{g}}_{m,k} \triangleq \mathbf{g}_{mk} - \hat{\mathbf{g}}_{m,k}$ as the channel estimation error. By considering random realizations of the MMSE channel estimate and the channel estimation error during an arbitrary coherence block, it holds true that $\hat{\mathbf{g}}_{m,k}$ and $\tilde{\mathbf{g}}_{m,k}$ are uncorrelated and are respectively distributed as [7].

$$\hat{\mathbf{g}}_{m,k} \sim \mathcal{CN} \left(0, \frac{\tau\rho_p \beta_{mk}^2}{\tau\rho_p \sum_{j=1}^K \beta_{mj} |\Phi_k^H \Phi_j|^2 + 1} I_N \right)$$

$$\tilde{\mathbf{g}}_{m,k} \sim \mathcal{CN} \left(0, \left(\beta_{mk} - \frac{\tau\rho_p \beta_{mk}^2}{\tau\rho_p \sum_{j=1}^K \beta_{mj} |\Phi_k^H \Phi_j|^2 + 1} \right) I_N \right) \quad (4)$$

ii. Downlink data transmission

The downlink signal intended to each user is precoded at the APs with conjugate beamforming. Accordingly, the transmit signal of the m^{th} AP to all users is

$$\mathbf{y}_{m,d} = \sqrt{\rho_d} \sum_{j=1}^K \sqrt{\eta_{mk}} \hat{\mathbf{g}}_{m,k}^* x_k \quad (5)$$

where x_k with $\mathbb{E}\{|x_k|^2\} = 1$, denotes the data symbol intended for user k , ρ_d accounts for the downlink transmit

power and η_{mk} , the power coefficient between from the m^{th}

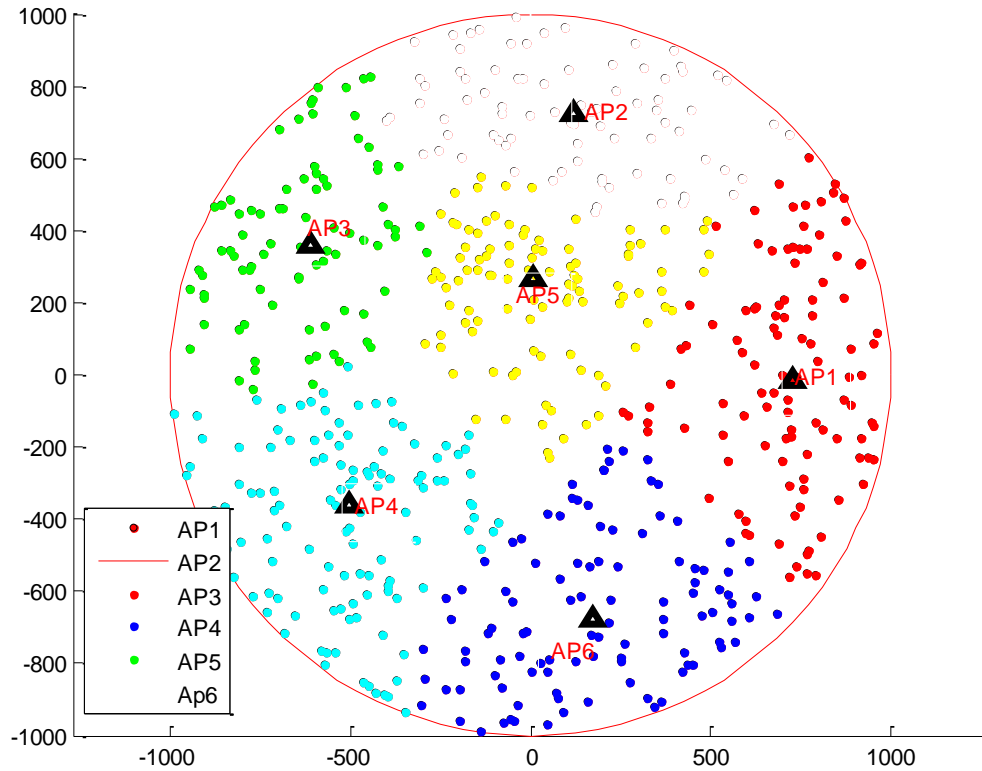


Figure-2: System Model for Cell Free Massive MIMO Network

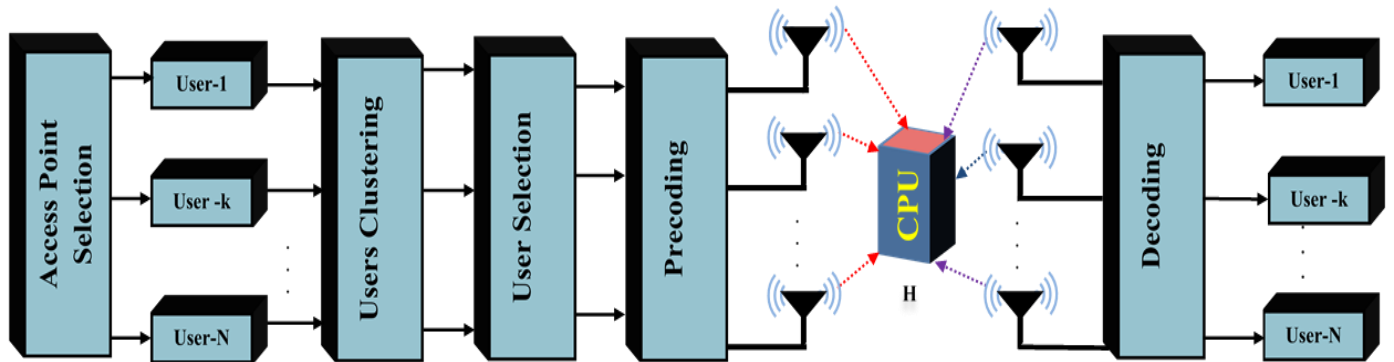


Fig.3. Systematic Block Diagram of our Proposed Cell Free Massive MIMO System

AP to user k chosen to satisfy $\mathbb{E}\{\|\mathbf{y}_{m,d}\|^2\} \leq \rho_d$, at each AP. The received signal at the k^{th} user is given by

$$\mathbf{r}_k = \sqrt{\rho_d} \sum_{m=1}^M \sum_{j=1}^K \sqrt{\eta_{mj}} \mathbf{g}_{mk}^T \hat{\mathbf{g}}_{m,j}^* d_j + \boldsymbol{\omega}_{m,k} \quad (6)$$

where $\boldsymbol{\omega}_{m,k} \sim \mathcal{CN}(0,1)$ denotes the AWGN at user k . Similarly, to [7], [9], we assume that users have only statistical knowledge of the channel estimate. Accordingly, the net downlink rate of the k^{th} user is given by [9].

$$R_k = B \left(1 - \frac{\tau}{T_c}\right) \times \log_2 \left(1 + \frac{\rho_d \left(\sum_{m=1}^M \sqrt{\eta_{mk}} N v_{mk}\right)^2}{N \rho_d \sum_{m=1}^M \eta_{mk} \beta_{mk} v_{mk} + N \rho_d \sum_{j \neq k}^K I_{kj}} + 1\right) \quad (7)$$

where B is the spectral bandwidth, $(1 - \frac{\tau}{T_c})$ is the fraction of the channel uses spent for downlink data transmission and

$$v_{mk} \triangleq \frac{\tau \rho_p \beta_{mk}^2}{\tau \rho_p \sum_{j=1}^K \beta_{mj} |\Phi_k^H \Phi_j|^2 + 1}$$

$$I_{kj} \triangleq N \left(\sum_{m=1}^M \sqrt{\eta_{mj}} \frac{v_{mj}}{\beta_{mj}} \beta_{mk} \right)^2 |\Phi_j^H \Phi_k|^2 + \sum_{m=1}^M \eta_{mj} v_{mj} \beta_{mk} \quad (8)$$

iii. Spectral Efficiency Derivation

In the uplink information transmission training phase, we define a set of AP selection diagonal matrices D_k , where $D_k = \text{diag}(d_{1k}, \dots, d_{Mk})$. More precisely, the m^{th} diagonal element of D_k is 1 if the m^{th} AP is allowed to decode signals from user k , and it is 0 otherwise. Let s_k denote the symbol of the k^{th} user with $\mathbb{E}\{|s_k|^2\} = 1$. The m^{th} AP received signal vector is given by

$$\mathbf{z}_m^u = \sqrt{\rho_u} \sum_{k=1}^K \sqrt{\rho_k} \mathbf{h}_{mk} s_k + \boldsymbol{\omega}_m^u \quad (9)$$

where ρ_k , ($0 \leq \rho_k \leq 1$) is the power control coefficient, ρ_u denotes the normalized uplink SNR, and $\boldsymbol{\omega}_m^u \sim \mathbb{CN}(0, \sigma^2 \mathbf{I}_N)$. The signal is decoded in two layers. In the first layer of decoding, the m^{th} AP locally detects the useful signal of the k^{th} user through the conjugate transpose of its estimated channel, $\hat{\mathbf{h}}_{mk}^H$. Thus, the first-layer decoded signal at the m^{th} AP is

$$\tilde{r}_{mk} = \mathbf{z}_m^u \hat{\mathbf{h}}_{mk}^H = \sqrt{\rho_u} \sum_{k=1}^K \sqrt{\rho_k} \mathbf{h}_{mk} \hat{\mathbf{h}}_{mk}^H s_k + \hat{\mathbf{h}}_{mk}^H \boldsymbol{\omega}_m^u \dots \dots \dots (10)$$

$$SINR_k = \frac{|\sqrt{\rho_u \rho_k} \sum_{m=1}^M \alpha_{mk}^* d_{mk} \mathbb{E}\{\hat{\mathbf{h}}_{mk} \hat{\mathbf{h}}_{mk}^H\}|^2}{\mathbb{E}\left\{ \left| \sqrt{\rho_u \rho_k} \sum_{m=1}^M \alpha_{mk}^* d_{mk} \mathbf{h}_{mk} \hat{\mathbf{h}}_{mk}^H - \sqrt{\rho_u \rho_k} \sum_{m=1}^M \alpha_{mk}^* d_{mk} \mathbb{E}\{\hat{\mathbf{h}}_{mk} \hat{\mathbf{h}}_{mk}^H\} \right|^2 \right\} + \sum_{k \neq k}^K \mathbb{E}\left\{ \left| \sqrt{\rho_u \rho_k} \sum_{k=1}^K \alpha_{mk}^* d_{mk} (\hat{\mathbf{h}}_{mk}^H (e_{m\hat{k}} + \hat{\mathbf{h}}_{m,\hat{k}})) \right|^2 \right\} + \mathbb{E}\left\{ \left| \sum_{m=1}^M \alpha_{mk}^* d_{mk} \hat{\mathbf{h}}_{mk}^H \boldsymbol{\omega}_m^u \right|^2 \right\}} \quad (12)$$

$$SINR_k = \frac{|\mathbf{S}_1|^2}{\mathbb{E}\{|\mathbf{S}_2|^2\} + \sum_{k \neq k}^K \mathbb{E}\{|\mathbf{S}_3|^2\} + \mathbb{E}\{|\mathbf{S}_4|^2\}} \quad (13)$$

where \mathbf{S}_1 , \mathbf{S}_2 , \mathbf{S}_3 , and \mathbf{S}_4 represent the strength of the desired signal, the beamforming gain uncertainty, the interference from user \hat{k} , and the noise. Due to the properties of MMSE estimation, the channel estimate $\hat{\mathbf{h}}_{mk}$ and the channel estimation error $e_{m\hat{k}}$ are uncorrelated. Thus, we can get

$$\mathbf{S}_1 = \sqrt{\rho_u \rho_k} \sum_{m=1}^M \alpha_{mk}^* d_{mk} \mathbb{E}\{\mathbf{h}_{mk} \hat{\mathbf{h}}_{mk}^H\}$$

The CPU receives the first-layer decoded signal and performs the second-layer decoding by computing the large-scale fading decoding (LSFD) weighted signal [12] involving a subset of the APs. The second-layer decoded signal received and processed at the CPU is

$$\hat{\mathbf{r}}_k = \sum_{m=1}^M \hat{\mathbf{h}}_{mk}^H \alpha_{mk}^* d_{mk} \mathbf{z}_m^u$$

$$\hat{\mathbf{r}}_k = \sum_{m=1}^M \hat{\mathbf{h}}_{mk}^H \alpha_{mk}^* d_{mk} \left(\sqrt{\rho_u} \sum_{k=1}^K \sqrt{\rho_k} \mathbf{h}_{mk} s_k + \boldsymbol{\omega}_m^u \right)$$

$$\hat{\mathbf{r}}_k = \sum_{m=1}^M \sqrt{\rho_u \rho_k} \alpha_{mk}^* d_{mk} \hat{\mathbf{h}}_{mk}^H \mathbf{h}_{mk} s_k + \sum_{m=1}^M \sum_{\substack{k=1 \\ k \neq k}}^K \sqrt{\rho_u \rho_k} \alpha_{mk}^* d_{mk} \hat{\mathbf{h}}_{mk}^H \mathbf{h}_{mk} s_k + \sum_{m=1}^M \alpha_{mk}^* d_{mk} \hat{\mathbf{h}}_{mk}^H \boldsymbol{\omega}_m^u \quad (11)$$

where α_{mk} is the complex LSFD coefficient for AP m and user k . The inter-user interference is reduced by using the LSFD coefficient. The AP selection coefficient d_{mk} reduces the burden of the fronthaul link by allowing only some of the APs to participate in signal detection. Hence, the signal to interference plus noise ratio (SINR) of k^{th} users of the system is

$$\mathbf{S}_1 = \sqrt{\rho_u \rho_k} \sum_{m=1}^M \alpha_{mk}^* d_{mk} \mathbb{E}\{\hat{\mathbf{h}}_{mk} \hat{\mathbf{h}}_{mk}^H\} \quad (14)$$

$$\mathbf{S}_2 = \sqrt{\rho_u \rho_k} \sum_{m=1}^M \alpha_{mk}^* d_{mk} (\mathbf{h}_{mk} \hat{\mathbf{h}}_{mk}^H - \mathbb{E}\{\hat{\mathbf{h}}_{mk} \hat{\mathbf{h}}_{mk}^H\})$$

$$\mathbf{S}_3 = \sqrt{\rho_u \rho_k} \sum_{m=1}^M \alpha_{mk}^* d_{mk} \mathbf{h}_{mk} \hat{\mathbf{h}}_{mk}^H - \sqrt{\rho_u \rho_k} \sum_{m=1}^M \alpha_{mk}^* d_{mk} \mathbb{E}\{\hat{\mathbf{h}}_{mk} \hat{\mathbf{h}}_{mk}^H\} \quad (15)$$

We have $e_{mk} = \mathbf{h}_{mk} - \hat{\mathbf{h}}_{m,k}$ so $\mathbf{h}_{mk} = e_{mk} + \hat{\mathbf{h}}_{m,k}$, therefore using equation (14), equation (15) can be written as

$$S_2 = \sqrt{\rho_u \rho_k} \sum_{m=1}^M \alpha_{mk}^* d_{mk} \hat{\mathbf{h}}_{mk}^H (\mathbf{e}_{mk} + \hat{\mathbf{h}}_{m,k}) - S_1 \quad (16)$$

$$S_3 = \sqrt{\rho_u \rho_k} \sum_{k=1}^K \alpha_{mk}^* d_{mk} \mathbf{h}_{mk} \hat{\mathbf{h}}_{mk}^H \quad (17)$$

We have $\mathbf{e}_{m\hat{k}} = \mathbf{h}_{m\hat{k}} - \hat{\mathbf{h}}_{m,\hat{k}}$ so $\mathbf{h}_{m\hat{k}} = \mathbf{e}_{m\hat{k}} + \hat{\mathbf{h}}_{m,\hat{k}}$, therefore equation (17) can be written as

$$S_3 = \sqrt{\rho_u \rho_k} \sum_{k=1}^K \alpha_{mk}^* d_{mk} (\hat{\mathbf{h}}_{mk}^H (\mathbf{e}_{m\hat{k}} + \hat{\mathbf{h}}_{m,\hat{k}})) \quad (18)$$

$$S_4 = \sum_{m=1}^M \alpha_{mk}^* d_{mk} \hat{\mathbf{h}}_{mk}^H \mathbf{w}_m^u \quad (19)$$

The lower bound on the uplink ergodic SE for the k^{th} user with the LSFD and AP selection coefficient is

$$SE_k = \frac{\tau_u}{\tau_c} \times \sum_{k=1}^K \log_2(1 + SINR_k)$$

$$SE_k = \frac{\tau_u}{\tau_c} \times \sum_{k=1}^K \log_2 \left(1 + \frac{|\sqrt{\rho_u \rho_k} \sum_{m=1}^M \alpha_{mk}^* d_{mk} \mathbb{E}\{\hat{\mathbf{h}}_{mk} \hat{\mathbf{h}}_{mk}^H\}|^2}{\mathbb{E}\left\{\left|\sqrt{\rho_u \rho_k} \sum_{m=1}^M \alpha_{mk}^* d_{mk} \mathbf{h}_{mk} \hat{\mathbf{h}}_{mk}^H - \sqrt{\rho_u \rho_k} \sum_{m=1}^M \alpha_{mk}^* d_{mk} \mathbb{E}\{\hat{\mathbf{h}}_{mk} \hat{\mathbf{h}}_{mk}^H\}\right|^2\right\} + \sum_{k \neq \hat{k}}^K \mathbb{E}\left\{\left|\sqrt{\rho_u \rho_k} \sum_{k=1}^K \alpha_{mk}^* d_{mk} (\hat{\mathbf{h}}_{mk}^H (\mathbf{e}_{m\hat{k}} + \hat{\mathbf{h}}_{m,\hat{k}}))\right|^2\right\} + \mathbb{E}\left\{\left|\sum_{m=1}^M \alpha_{mk}^* d_{mk} \hat{\mathbf{h}}_{mk}^H \mathbf{w}_m^u\right|^2\right\}} \right) \quad (20)$$

The effective SINR of user k in (13) with the LSFD and AP selection coefficient can be rewritten as-

$$SINR_k = \frac{|\sqrt{\rho_u \rho_k} \mathbf{u}_k^H \mathbf{v}_k|^2}{\mathbf{u}_k^H (\sum_{k=1}^K \rho_u \rho_k \mathbf{W}_{kk}) \mathbf{u}_k - \rho_u \rho_k |\mathbf{u}_k^H \mathbf{v}_k|^2 + \mathbf{u}_k \mathbf{u}_k^H \mathbf{X}_k}$$

$$SINR_k = \frac{\rho_u \rho_k |\mathbf{u}_k^H \mathbf{v}_k|^2}{\mathbf{u}_k^H (\sum_{k=1}^K \rho_u \rho_k \mathbf{W}_{kk}) \mathbf{u}_k - \rho_u \rho_k |\mathbf{u}_k^H \mathbf{v}_k|^2 + \mathbf{u}_k \mathbf{u}_k^H \mathbf{X}_k} \quad (21)$$

where $\mathbf{u}_k = \text{diag}(\mathbf{A}_k \mathbf{D}_k)$, $\mathbf{A}_k = \text{diag}(\alpha_{1,k}, \dots, \alpha_{M,k})$, and $\mathbf{u}_{mk} = \alpha_{mk} d_{mk}$. $\mathbf{v}_k \triangleq [\mathbf{v}_{1k}, \dots, \mathbf{v}_{Mk}]^T$. \mathbf{X}_k is a diagonal matrix, and its m^{th} diagonal element is $x_{mk} = \sigma^2 \text{tr}(\hat{\mathbf{R}}_{mk})$. $w_{kk}^{m\hat{m}}$ is the $(m, \hat{m})^{\text{th}}$ element of the matrix $\mathbf{W}_{k\hat{k}}$. The elements of \mathbf{v}_k and $\mathbf{W}_{k\hat{k}}$ are given as

$$\mathbf{v}_{mk} = \mathbb{E}\{\hat{\mathbf{h}}_{mk} \hat{\mathbf{h}}_{mk}^H\}$$

$$\mathbf{v}_{mk} = \tau \rho_p \Phi_{mk}^{-1} \mathbf{R}_{mk} \mathbf{h}_{mk}^- \mathbf{h}_{mk}^{-H} + \tau \rho_p \beta_{mk} (\Phi_{mk}^{-1} \mathbf{R}_{mk}) \quad (22)$$

$$w_{kk}^{m\hat{m}} = \mathbb{E}\{\hat{\mathbf{h}}_{mk}^H \mathbf{h}_{mk} \mathbf{h}_{mk}^H \hat{\mathbf{h}}_{mk}\}$$

$$w_{kk}^{m\hat{m}} = \mathbb{E}\{\hat{\mathbf{h}}_{mk}^H (\mathbf{e}_{m\hat{k}} + \hat{\mathbf{h}}_{m,\hat{k}})^H (\mathbf{e}_{m\hat{k}} + \hat{\mathbf{h}}_{m,\hat{k}}) \hat{\mathbf{h}}_{mk}\}$$

$$w_{kk}^{m\hat{m}} = \begin{cases} 2\tau^2 \rho_p^2 \beta_{mk} \times \Re\{\Phi_{mk}^{-1} \mathbf{R}_{mk} \mathbf{h}_{mk}^- \mathbf{h}_{mk}^{-H} \times \text{tr}(\Phi_{mk}^{-1} \mathbf{R}_{mk})\} \\ \quad + \tau^2 \rho_p^2 \beta_{mk}^2 |\text{tr}(\Phi_{mk}^{-1} \mathbf{R}_{mk})|^2 \\ \quad + \tau \rho_p \text{tr}(\Phi_{mk}^{-1} \mathbf{R}_{mk} \mathbf{R}_{mk} \mathbf{R}_{mk}) & \hat{k} \in \mathcal{P}_k \\ \text{tr}(\hat{\mathbf{R}}_{mk} \mathbf{R}_{m\hat{k}}) & \hat{k} \notin \mathcal{P}_k \end{cases} \quad (23)$$

To reduce the pressure of the fronthaul link while considering the spectral efficiency of the system, we investigate a joint optimization problem involving user grouping, user scheduling and access point selection. However, the joint optimization problem involves access point selection and is an integer optimization problem, which increases the complexity of system processing. To reduce the complexity of system optimization processing, we use ZF and MMSE precoding techniques. A suboptimal access point selection (APS) algorithm based on the maximum channel gain is proposed.

III. Linear precoding

We consider two linear precoding schemes that are used for the analysis of SE of the cell free Massive MIMO system. Precoding is a method in which by multiplying the precoding matrixes with user data capable to suppress the interference of the system that is produced due to the signals of other users [13]. From equation (10), the precoding scheme is shown in Fig.4.

CF M-MIMO system equipped with M APs and N users both having a single antenna used for transmission and reception of information data. In this system, ZF and MMSE precoding is used for suppression of IUI for $M \geq N$.

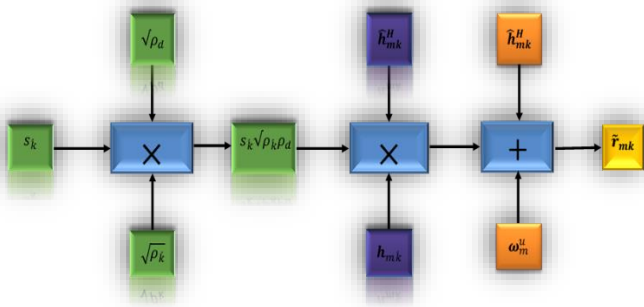


Fig.4. Block diagram of Precoding Scheme

i. Zero-Forcing (ZF) Precoding

ZF precoding is a linear precoding scheme. This precoding scheme is designed in such a way so that it completely mitigates the IUI of each user. Let, k^{th} user precoding weighted matrix is W_k . This precoding scheme eliminate the interference to zero, such that

$$g_k W_j = 0 \quad \text{for } j \neq k \dots \dots (24)$$

Hence, equation (9) may be rewritten as

$$\tilde{r}_{mk} = \underbrace{\sqrt{\rho_u} \sum_{k=1}^K \sqrt{\rho_k} h_{mk} \hat{h}_{mk}^H s_k}_{\text{desired signal}} + \underbrace{\hat{h}_{mk}^H \omega_m^u}_{\text{AWGN}} \dots \dots (25)$$

where the Moore-Penrose pseudo-inverse of ZF precoding scheme which is given below-

$$W_{ZF} = g^\dagger = g^H (g g^H)^{-1} \dots \dots (26)$$

Hence, the achievable SE of the CF M-MIMO system is obtained from equation (25) after the application of the ZF precoding scheme is given as

$$R_{ZF,k} = \sum_{n=1}^N \log_2(1 + SINR_k)$$

$$R_{ZF,k} = \sum_{n=1}^N \log_2 \left(1 + \frac{\left| \sqrt{\rho_u} \sum_{k=1}^K \sqrt{\rho_k} h_{mk} \hat{h}_{ZF,k}^H s_k \right|^2}{\left| \sqrt{\rho_u} \sum_{j=1, j \neq k}^K \sqrt{\rho_j} h_{mj} \hat{h}_{ZF,j}^H s_j \right|^2 + \hat{h}_{ZF,k}^H \omega_m^u} \right) \dots (27)$$

ii. Minimum Mean Square Error (MMSE) Precoding

The MMSE is another type of linear precoding scheme that cannot eliminate interference rather it can offer a good trade-off between the noise improvement and suppression of interference. The MMSE estimator follows an estimation method through which it can reduce the mean square error. The post-detection SINR maximization the MMSE precoding weighted matrix is given by

$$W_{MMSE} = g^H \left(g g^H + \frac{\sigma^2 I}{\rho_{dl}} \right)^{-1} \dots \dots (28)$$

where σ^2 is the variance of noise power. We assume the channel has a imperfect CSI and I am the identity matrix. The k^{th} achievable SE of CF M-MIMO system is obtained from equation (9) after the application of the MMSE precoding scheme which is given below-

$$R_{MMSE,k} = \sum_{n=1}^N \log_2 \left(1 + \frac{\left| \sqrt{\rho_u} \sum_{k=1}^K \sqrt{\rho_k} h_{mk} \hat{h}_{MMSE,k}^H s_k \right|^2}{\left| \sqrt{\rho_u} \sum_{j=1, j \neq k}^K \sqrt{\rho_j} h_{mj} \hat{h}_{MMSE,j}^H s_j \right|^2 + \hat{h}_{MMSE,k}^H \omega_m^u} \right) \dots (29)$$

IV. User Grouping Method

In this paper, N numbers of users are divided into G cluster using a simple K -means clustering method. These clusters separated the users into six different parts surrounding the APs as shown in Fig.1 and Fig.2. When large numbers of users are separated into groups, the channel matrix size of each group is becoming very small; hence, the computational complexity of the algorithm is reduced. The steps of K -means users clustering and grouping algorithm is presented in below-

Initialization:

1. The number of clusters, $G=6$.
2. Randomly choose G number of centroids on the cell around the APs and then randomly selecting users for each centroid.

Repeat

3. Re-assign each user to the cluster to which the user is to the closest cluster, based on the mean value of the users in the cluster.
4. Keep iterating until there no change to the users.

End

5. G numbers of clusters are formed around the APs.

V. User Selection Algorithm

In this paper, we consider the semi-orthogonal user selection (SUS) algorithm for the system performance analysis in the CF M-MIMO system. From N users, S users are selected from G clusters using the SUS algorithm. The steps of this algorithm are described below.

Semi-orthogonal User Selection (SUS) Algorithm

1. Total no of APs= M ;
2. Total no of User N ;
3. Iteration $i \leftarrow 1$;
4. $\Delta \leftarrow \{1,2, \dots, N\}$ is the set of all users

5. $S_S \leftarrow \phi$ is the set of selected users from all clusters.
6. $S_1 = \operatorname{argmax}_{k \in \Delta} \|\mathbf{H}_{S,A}\|_F^2$ the first set of user-select
7. $S_S \leftarrow S_S \cup S_1$;
8. while $i < S$
9. For each k in Δ do
10. $\frac{|\mathbf{H}_k^H \mathbf{H}_{k-1}|}{\|\mathbf{H}_k\| \|\mathbf{H}_{k-1}\|} \leq \phi$ for orthogonality test between the users.
11. end
12. $\Omega_S = \operatorname{argmax}_{k \in \Delta} \|\mathbf{H}_{k,A}\|_F^2$
13. Update $S_S \leftarrow S_S \cup \Omega_S$; $\Delta \leftarrow \Delta \setminus \Omega_S$
14. $\mathbf{H}_S = \mathbf{H}_{S,A}$ Set of Channel vector of the selected user
15. $i = i + 1$
16. end
17. Repeat the process from step 8 to 16 till S users are selected from all clusters.
18. $S_{SUS} = S_S$

VI. Access Point Selection (APS) Algorithm

Access Point Selection is performing after the user scheduling scheme. In this paper, the S number of APs are selected from M APs for transmission of data. In our access point selection (APS) algorithm, at every step, from S selected users a particular user is considered. The channel is assumed as a reciprocal and maximum channel gain-based APS algorithm is considered to select a set of S AP from M APs which corresponds to the strongest orthogonal channel from the user to the AP to schedule with selected users set. The data in regards to the index of the selected AP is then sent to the CPU. Lastly, the CPU update the set of available transmits APs to the next user in order. Thus, the selected users are allocated with the set of transmit AP.

Access Point Selection (APS) Algorithm based on maximum channel gain:

1. For each user in S_{SUS} , $\mathbf{H}_S = \mathbf{H}_{S,A}$ set of channel vector of the selected user
2. Number of AP M ;
3. Iteration $j \leftarrow 1$;
4. $A \leftarrow \{1, \dots, m, \dots, M\}$ is the set of all AP.
5. $S_{S,S} \leftarrow \phi$ is the set of the selected AP.
6. while $j \leq A$
7. $S_A = \operatorname{argmax}_{i \in A} \|\mathbf{H}_{S,i}\|_F^2$
8. Update $S_{S,S} \leftarrow S_{S,S} \cup S_A$; $A \leftarrow A \setminus S_{S,S}$;
9. $\mathbf{H}_{S,S} = \mathbf{H}_{S,i}$ Set of Channel vector of selected user and AP
10. $j \leftarrow j + 1$
11. end
12. Repeat the process from step 6 to 10 till S number of APs are selected.
13. $S_{S,S} = S_{SUS-AS}$

VII. Analysis of Computational Complexity of SUS Algorithms

In this section, we quantify the computational complexity of the SUS algorithms. Moreover, we compare the computational complexity of our SUS algorithm with other SUS algorithms that are shown in table-1. Generally, computational complexity of an algorithm is quantified in terms of flop counts as expressed as ϕ . A flop count for a given matrix computation is

computed by summing real addition, subtraction, multiplication and division associated with each step of the algorithm. A flop is equivalent to a real floating-point operation, a complex addition is equivalent to two flops, and one complex multiplication is equivalent to six flops [14]. The actual calculation of flops slightly differs from the actual complexity computation. In this paper, the number of scheduled users is very much less than the number of total users, i.e. $1 \leq s \leq N$.

A. The Complexity of SUS Algorithm

The calculation of flops in SUS algorithm starts from iteration $n=1$ to N . In each iteration, a newly selected semi-orthogonal user is added to the set containing earlier chosen users. In each iteration, new users which are semi orthogonal to the users in the set are found and from which the one with the largest channel vector norm is kept and added to the set, with $(nN)^2 M$ flops. The algorithm terminates when the specified number of semi-orthogonal users are selected. The final expression of ϕ is as shown below.

$$\phi = \frac{1}{G} \left\{ 4NM - N + \sum_{n=1}^M [N + \{M(16n - 12) - 2n + 2\} + \{(12M + 1)(N - 1) + N\}] \right\}$$

$$\phi = \frac{1}{G} \left\{ 4NM - N + MN + \frac{16M^2(M + 1)}{2} - 12M^2 - \frac{2M(M + 1)}{2} + 2M + (12M^2 + M)(N - 1) + NM \right\}$$

$$\phi = \frac{1}{G} \{ 7NM - N + 8M^3 - 17M^2 + 12NM^2 \}$$

$$\phi = \frac{1}{G} \{ O(NM^2) \}$$

Hence complexity of our modified SUS algorithm is $O(NM^2)$.

Table-1: Complexity Comparison of SUS algorithms

Reference	Complexity
Reference [15]	$\approx O(N^3)$
Reference [16]	$\approx O\left(\frac{K}{3} \bar{K}^4 N^3\right)$
Proposed SUS Algorithm	$\approx \frac{1}{G} O(M^2 N)$

From the table-1 it is shown that the computation complexity of our considered SUS algorithm is very small compared to the other existing SUS algorithms.

VIII. RESULTS AND DISCUSSION

In this section, we study the performance of an CF M-MIMO system by simulation in MATLAB. We consider the user clustering as explained above; users are semi-orthogonal amongst each other in the individual cluster and also semi-orthogonal among all clusters. We assume the following

parameters shown in table-2. As said above, we consider ZF and MMSE precoding with Rayleigh fading channel, and the system with variation in SNR values. The corresponding numbers of S APs are selected based on maximum SNR for a given selected user as explained in the algorithm. The circular service area is divided into equal circular zones so that each zone expected to be contains the approximately equal number of users.

Table2: Values of Parameters use during Simulation

Parameters name	values
Total no of Users (N)	256
Total no of AP (M)	36
Total no of clusters (G)	6
Total Selected number of users and AP (S)	6
Path loss (L)	3.8
The radius of the circular service area (r)	1000
AWGN (ω)	-90dBm
Bandwidth	20MHz
Shadow fading variable with standard deviation is (σ_{shadow})	8 dB
ρ_p, ρ_u, ρ_d	200mW
ϕ	0.1
τ, τ_c, τ_u	20,200,190

As we simulate the system assuming 20 MHz is the bandwidth of the system. For the simulation of a practical Cell Free Massive MIMO system, the algorithm is run for large times, and the average value of the system sum-rate and individual rate is obtained. In Fig. 5 we show the results for $S=6$ where we varied the received SNR of the users, and considering ZF and MMSE precoding. The trend of sum-rate of all precoding schemes are the same. We observed that the system rate is highest for ZF and MMSE is little bit lower.

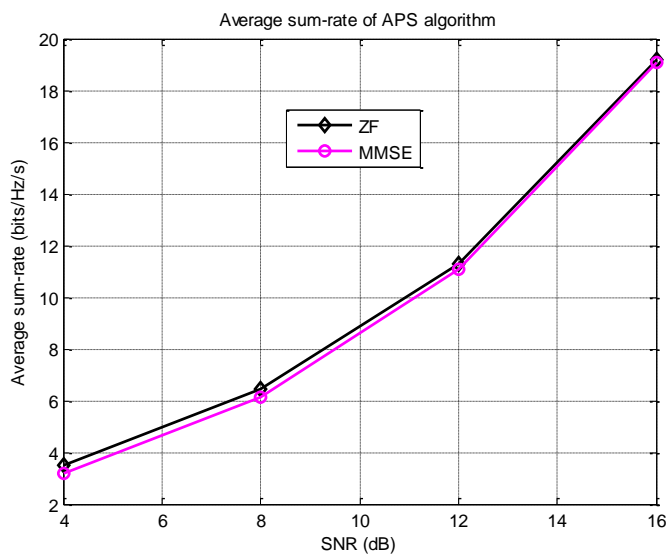


Figure-5(a): Average sum-rate of APS algorithm of all the APs using ZF and MMSE precoding.

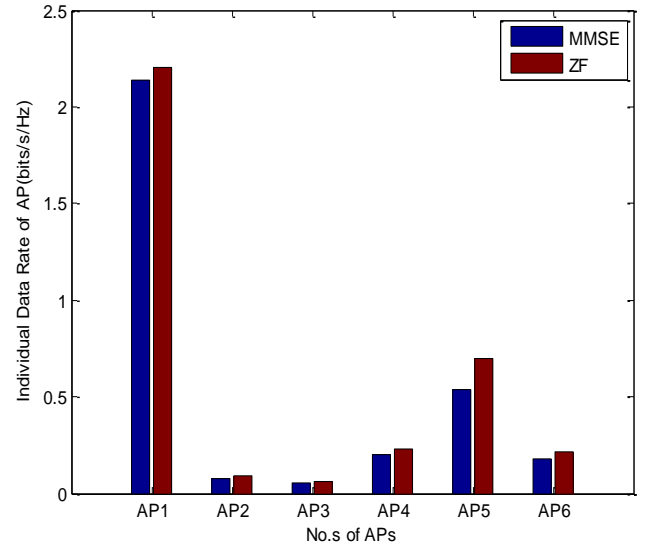


Figure-5(b): Highest individual data-rate of AP1.

Figure-5(a) shows the average system sum-rate of APS algorithm with ZF and MMSE precoding schemes. The average system sum-rate of the ZF and MMSE is increases with increase of transmit SNR. The average sum-rate difference between ZF and MMSE precoding scheme is very small and when SNR value increases the sum-rate differences are become very small. The average sum-rate is more in ZF compare to the MMSE precoding scheme that is shown in figure-5(a). This analysis is done when we found the highest individual rate in AP-1.

Figure-5(b) shows the individual rate of all the APs at 4dB transmit SNR. It is noticed from figure-5(b) that the rate of individual APs is varies. Some APs provide more rate and some one very less. In Figure-5(b) AP-1 provide maximum rate compare to the other APs. It also explored that with ZF precoding scheme achieved higher rate than MMSE precoding scheme.

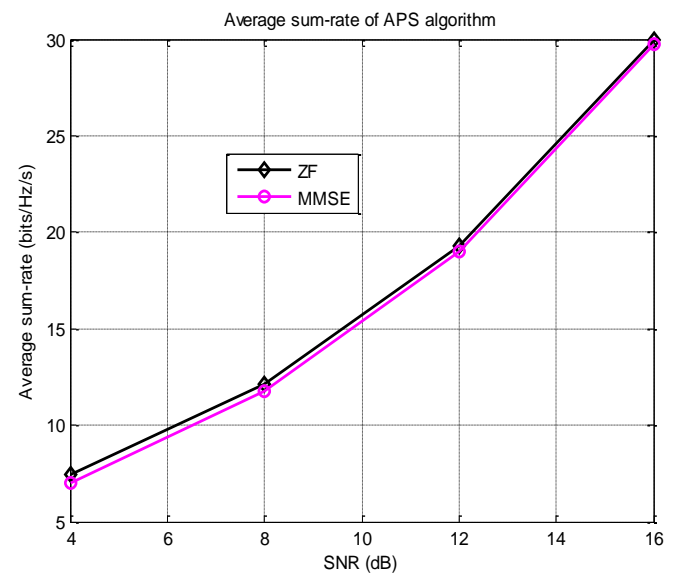


Figure-6(a): Average sum-rate of APS algorithm of all the APs using ZF and MMSE precoding.

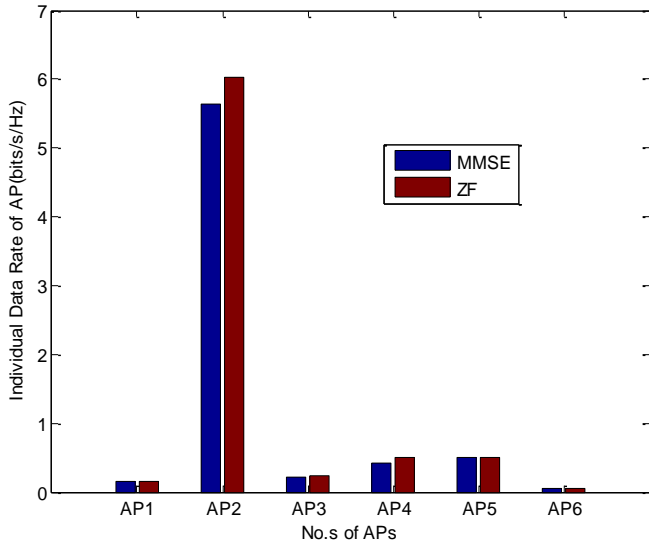


Figure-6(b): Highest individual data-rate of AP-2.

Figure-6(a) shows the average system sum-rate of APS algorithm with ZF and MMSE precoding schemes. The average system sum-rate of the ZF and MMSE is increases with increase of transmit SNR. The average sum-rate difference between ZF and MMSE precoding scheme is very small and when SNR value increases the sum-rate differences are become very small. The average sum-rate is more in ZF compare to the MMSE precoding scheme that is shown in figure-6(a). This analysis is done when we found the highest individual rate in AP-2.

Figure-6(b) shows the individual rate of all the APs at 4dB transmit SNR. It is noticed from figure-6(b) that the rate of individual APs is varies. Some APs provide more rate and some one very less. In Figure-6(b) AP-2 provide maximum rate compare to the other APs. It also explored that with ZF precoding scheme achieved higher rate than MMSE precoding scheme.

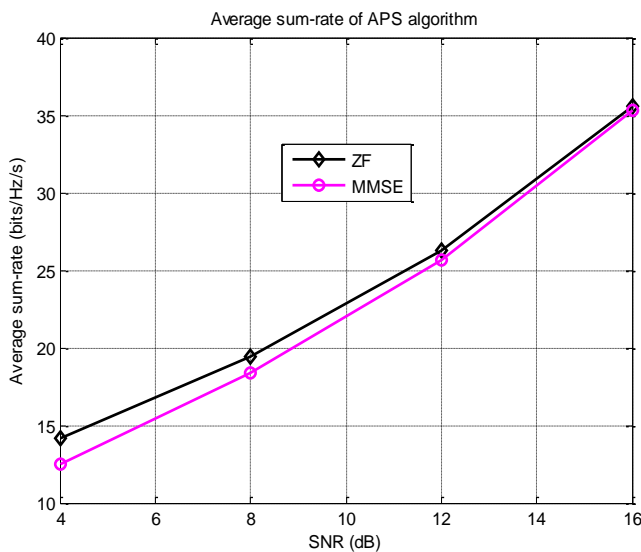


Figure-7(a): Average sum-rate of APS algorithm of all the APs using ZF and MMSE precoding.

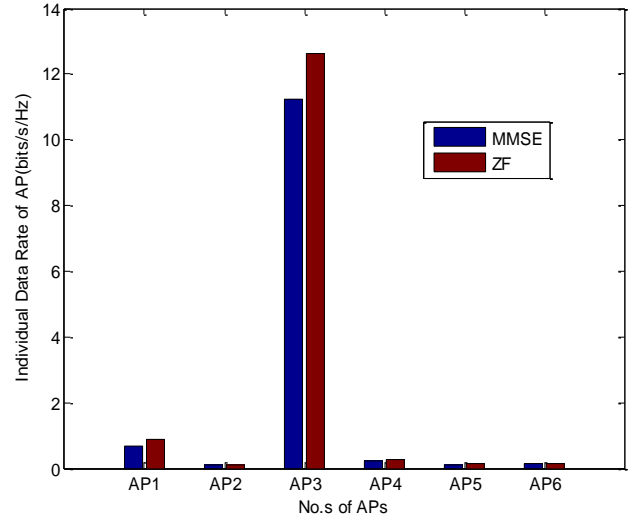


Figure-7(b): Highest individual data-rate of AP-3.

Figure-7(a) shows the average system sum-rate of APS algorithm with ZF and MMSE precoding schemes. The average system sum-rate of the ZF and MMSE is increases with increase of transmit SNR. The average sum-rate difference between ZF and MMSE precoding scheme is very small and when SNR value increases the sum-rate differences are become very small. The average sum-rate is more in ZF compare to the MMSE precoding scheme that is shown in figure-7(a). This analysis is done when we found the highest individual rate in AP-3.

Figure-7(b) shows the individual rate of all the APs at 4dB transmit SNR. It is noticed from figure-7(b) that the rate of individual APs is varies. Some APs provide more rate and some one very less. In Figure-7(b) AP-3 provide maximum rate compare to the other APs. It also explored that with ZF precoding scheme achieved higher rate than MMSE precoding scheme.

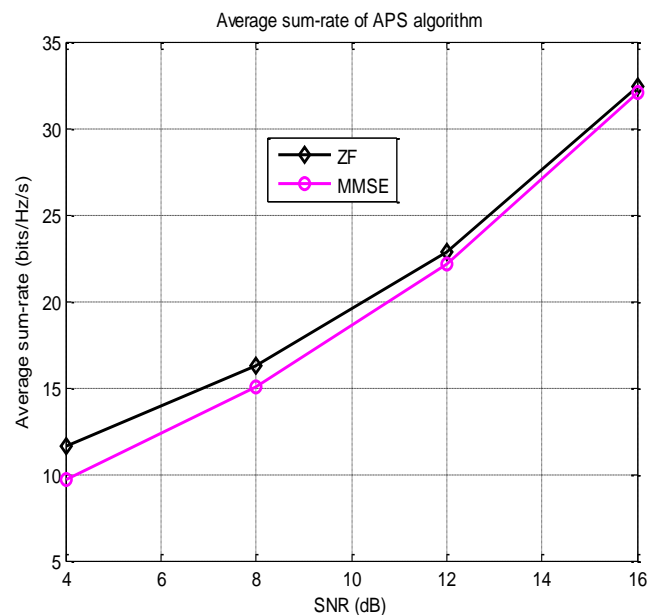


Figure-8(a): Average sum-rate of APS algorithm of all the APs using ZF and MMSE precoding.

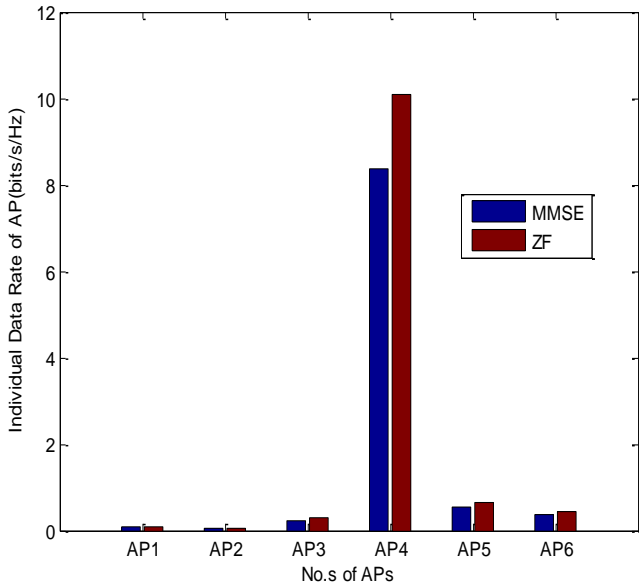


Figure-8(b): Highest individual data-rate of AP-4.

Figure-8(a) shows the average system sum-rate of APS algorithm with ZF and MMSE precoding schemes. The average system sum-rate of the ZF and MMSE is increases with increase of transmit SNR. The average sum-rate difference between ZF and MMSE precoding scheme is very small and when SNR value increases the sum-rate differences are become very small. The average sum-rate is more in ZF compare to the MMSE precoding scheme that is shown in figure-8(a). This analysis is done when we found the highest individual rate in AP-4.

Figure-8(b) shows the individual rate of all the APs at 4dB transmit SNR. It is noticed from figure-8(b) that the rate of individual APs is varies. Some APs provide more rate and some one very less. In Figure-8(b) AP-4 provide maximum rate compare to the other APs. It also explored that with ZF precoding scheme achieved higher rate than MMSE precoding scheme.

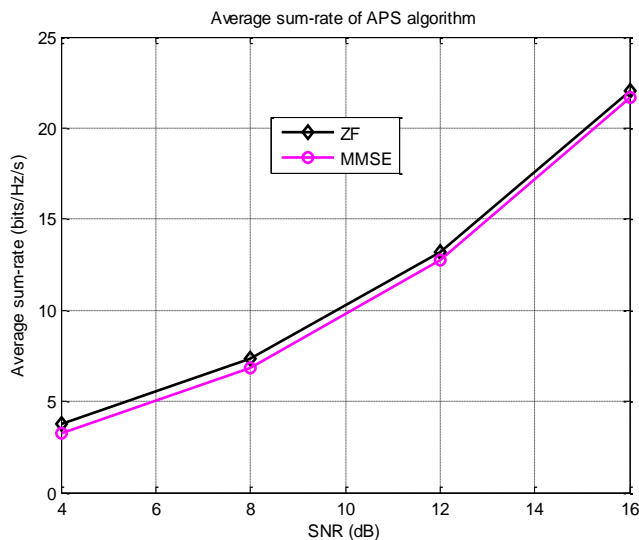


Figure-9(a): Average sum-rate of APS algorithm of all the APs using ZF and MMSE precoding.

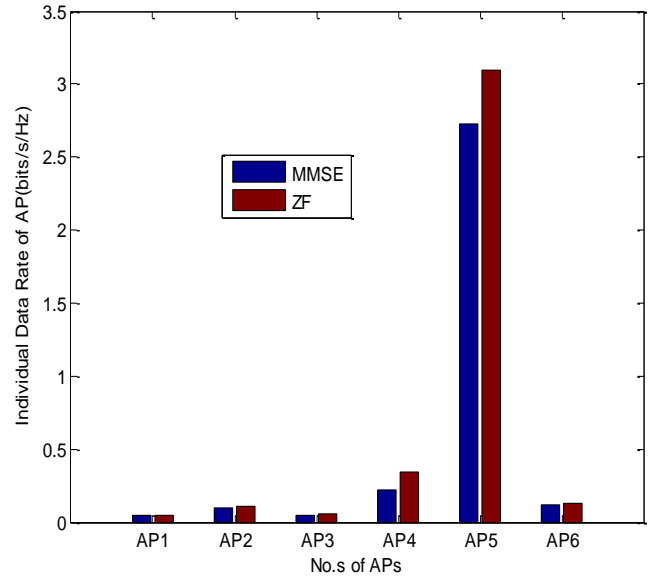


Figure-9(b): Highest individual data-rate of AP-5.

Figure-9(a) shows the average system sum-rate of APS algorithm with ZF and MMSE precoding schemes. The average system sum-rate of the ZF and MMSE is increases with increase of transmit SNR. The average sum-rate difference between ZF and MMSE precoding scheme is very small and when SNR value increases the sum-rate differences are become very small. The average sum-rate is more in ZF compare to the MMSE precoding scheme that is shown in figure-9(a). This analysis is done when we found the highest individual rate in AP-5.

Figure-9(b) shows the individual rate of all the APs at 4dB transmit SNR. It is noticed from figure-9(b) that the rate of individual APs is varies. Some APs provide more rate and some one very less. In Figure-9(b) AP-5 provide maximum rate compare to the other APs. It also explored that with ZF precoding scheme achieved higher rate than MMSE precoding scheme.

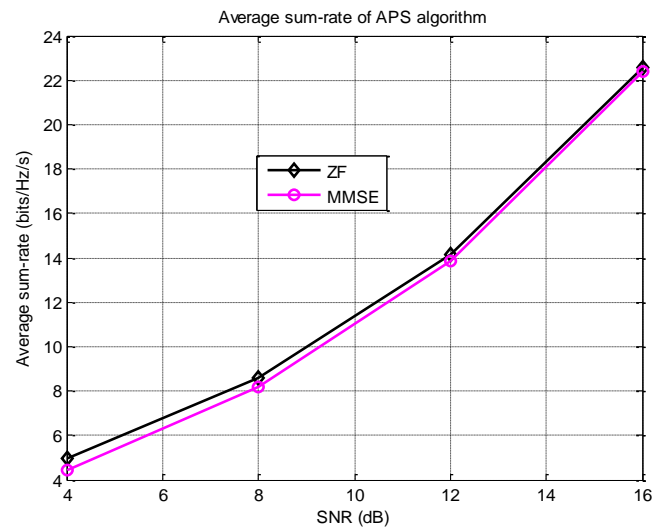


Figure-10(a): Average sum-rate of APS algorithm of all the APs using ZF and MMSE precoding.

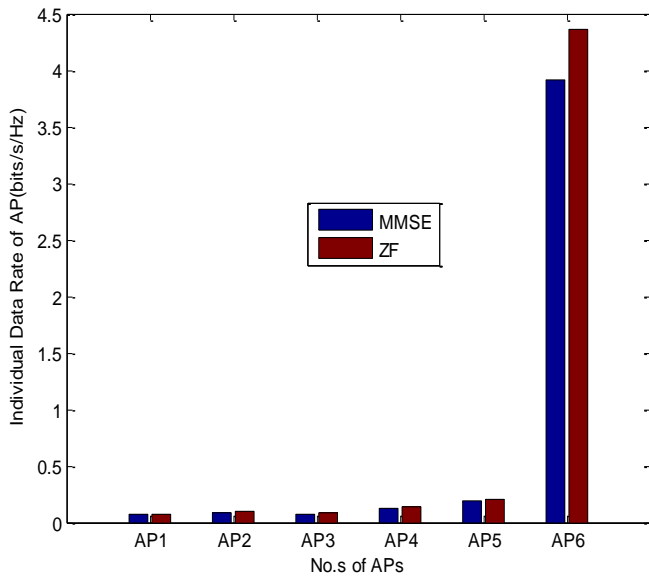


Figure-10(b): Highest individual data-rate of AP-6.

Figure-10(a) shows the average system sum-rate of APS algorithm with ZF and MMSE precoding schemes. The average system sum-rate of the ZF and MMSE is increases with increase of transmit SNR. The average sum-rate difference between ZF and MMSE precoding scheme is very small and when SNR value increases the sum-rate differences are become very small. The average sum-rate is more in ZF compare to the MMSE precoding scheme that is shown in figure-10(a). This analysis is done when we found the highest individual rate in AP-6.

Figure-10(b) shows the individual rate of all the APs at 4dB transmit SNR. It is noticed from figure-10(b) that the rate of individual APs is varies. Some APs provide more rate and some one very less. In Figure-10(b) AP-6 provide maximum rate compare to the other APs. It also explored that with ZF precoding scheme achieved higher rate than MMSE precoding scheme.

Conclusion

Cell Free massive MIMO equipped with large number of distributed access points (AP) which has potential to provide high data rate, spectral efficiency (SE), and energy efficiency (EE). The system performance of cell free M-MIMO is best when selected access points (AP) from large number of APs. In this work, we developed an Access Point Selection (APS) algorithm to maximize the system sum-rate with lower power consumption. With this APS algorithm we used zero-forcing (ZF) and minimum means square error (MMSE) precoding schemes used because it reduces the inter-user interference. Here, the maximum channel gain-based Access Point Selection (APS) algorithm is introduced for access point (AP) selection in cell free M-MIMO network to maximize the system performance. APS algorithm used to select those APs whose channel gain is highest therefore it improves the rate of the system. The same number of users is scheduled using simple semi-orthogonal user scheduling (SUS) algorithm. It is observed that the APS and SUS algorithm jointly improve the system rate significantly in cell free massive MIMO system.

We explored the system capacity of cell free massive MIMO system with 6 APs. The average system rate is also explored for different SNR values with ZF and MMSE precoding schemes. We observed that ZF precoding schemes provide maximum average sum rate where MMSE is minimum. We also analyzed the individual rate of APs at 4dB transmit SNR using ZF and MMSE precoding scheme. We have noticed from the results the rate of individual APs is not equals. Some APs provided higher rate some very low. From the result we have seen that our proposed algorithm successfully achieved the higher sum-rate.

Declaration

Funding: Department of Education of Guangdong Province Young Talents Project (2022KQNCX126).

Conflicts of interest/Competing interests : The authors have no conflict of interest regarding the paper.

Availability of data and material (data transparency): No

Code availability (software application or custom code): Custom code.

Authors' contributions: The major contributions of this paper summarized as follows:

- i. Using simple K -means clustering, a large number of users are separated into equal number of AP in the considered area.
- ii. Semi-orthogonality User Selection (SUS) algorithm is use to schedule the best users from each cluster.
- iii. Access Points are selected based on maximum channel gain.
- iv. ZF and MMSE linear precoding schemes are used to reduce interference and enhanced the system rate.

References

- [1] H. Q. Ngo, A. Ashikhmin, H. Yang, E. G. Larsson, and T. L. Marzetta, "Cell-free massive MIMO versus small cells," *IEEE Transaction Wireless Communication*, vol. 16, no. 3, pp. 1834-1850, Mar. 2017.
- [2] T. L. Marzetta, E. G. Larsson, H. Yang, and H. Q. Ngo, "Fundamentals of Massive MIMO" Cambridge, UK: Cambridge University Press, 2016.
- [3] E. Nayebi, A. Ashikhmin, T. L. Marzetta, H. Yang, and B. D. Rao, "Precoding and power optimization in cell-free massive MIMO systems," *IEEE Transaction on Wireless Communication*, vol. 16, no. 7, pp. 4445-4459, Jul. 2017.
- [4] G. Interdonato, H. Q. Ngo, E. G. Larsson, and P. Frenger, "How much do downlink pilots improve cell-free massive MIMO?" *IEEE Global Communication Conference (GLOBECOM)*, Washington, USA, pp.1-7, Dec. 2016.
- [5] Q. Huang and A. Burr, "Compute-and-forward in cell-free massive MIMO: Great performance with low backhaul load," *IEEE International Conference on Communication (ICC)*, Paris, France, pp.60-606, May 2017.

- [6] E. Bjornson, L. Sanguinetti, J. Hoydis, and M. Debbah, "Optimal design of energy-efficient multi-user MIMO systems: Is massive MIMO the answer?" *IEEE Transaction Wireless Communication*, vol. 14, no. 6, pp. 3059-3075, Jun. 2015.
- [7] E. Nayebi, A. Ashikhmin, T. L. Marzetta, and H. Yang, "Cell-Free Massive MIMO systems," *49th Asilomar Conference on Signals, Systems and Computers*, Nov. 2015, pp. 695–699.
- [8] S. M. Kay, "Fundamentals of Statistical Signal Processing: Estimation Theory," Upper Saddle River, NJ, USA: Prentice-Hall, Inc., 1993.
- [9] H. Q. Ngo, L. Tran, T. Q. Duong, M. Matthaiou and E. G. Larsson, "On the Total Energy Efficiency of Cell-Free Massive MIMO," *IEEE Transactions on Green Communications and Networking*, vol. 2, no. 1, pp. 25-39, March 2018.
- [10] T. L. Marzetta, "Noncooperative cellular wireless with unlimited numbers of base station antennas," *IEEE Transaction on Wireless Communication*, vol. 9, no. 11, pp. 3590-3600, Nov. 2010.
- [11] E. Björnson, J. Hoydis, M. Kountouris, and M. Debbah, "Massive MIMO Systems With Non-Ideal Hardware: Energy Efficiency, Estimation, and Capacity Limits," *IEEE Transaction on Information Theory*, vol. 60, no. 11, pp. 7112–7139, Nov. 2014.
- [12] T. Van Chien, C. Mollén, and E. Björnson, "Large-scale-fading decoding in cellular massive MIMO systems with spatially correlated channels," *IEEE Transaction on Communication*, vol. 67, no. 4, pp. 2746-2762, Apr. 2019.
- [13] T.A. Sheikh, J. Bora, and M.A. Hussain, "Performance of Data-Rate Analysis of Massive MIMO System Using User Grouping," *Wireless Personal Communication*, vol.116,no.1, pp. 455–474, 2021.
- [14] G. H. Golub and C. F. Van Loan, "Matrix Computations," 3rd Ed. Baltimore, MD: The John Hopkins Univ. Press, 1996.
- [15] B. Fang, Z.P. Qian, W.S., and W. Zhong, "RAISE: A New Fast Transmit Antenna Selection Algorithm for Massive MIMO System," *Wireless Personal Commun.*, vol. 80, no. 3, pp. 1147-1157, Feb. 2015.
- [16] K. Dong, N. Prasad, X.D. Wang, and S.H. Zhu, "Adaptive antenna selection and Tx/Rx beamforming for large-scale MIMO system in 60 GHz channels," *EUSIP Journal Wireless Commun. and Network.*, vol. 2011, no. 59, pp.1-14., 2011.